

BIOLOGICALLY INSPIRED ROBOT NAVIGATION BY EXPLOITING OPTICAL FLOW PATTERNS

Sotirios Ch. Diamantas*

*Intelligence, Agents, Multimedia Group, School of Electronics and Computer Science
University of Southampton, Southampton, SO17 1BJ, U.K.*

Anastasios Oikonomidis

Centre for Risk Research, School of Management, University of Southampton, Southampton, SO17 1BJ, U.K.

Richard M. Crowder

*Intelligence, Agents, Multimedia Group, School of Electronics and Computer Science
University of Southampton, Southampton, SO17 1BJ, U.K.*

Keywords: Optical flow, Biologically inspired robot navigation, Robot homing, Visual navigation, Mobile robotics.

Abstract: In this paper a novel biologically inspired method is addressed for the robot homing problem where a robot returns to its home position after having explored an *a priori* unknown environment. The method exploits the optical flow patterns of the landmarks and based on a training data set a probability is inferred between the current snapshot and the snapshots stored in memory. Optical flow, which is not a property of landmarks like color, shape, and size but a property of the camera motion, is used for navigating a robot back to its home position. In addition, optical flow is the only information provided to the system while parameters like position and velocity of the robot are not known. Our method proves to be effective even when the snapshots of the landmarks have been taken from varying distances and velocities.

1 INTRODUCTION

Recently there has been a resurgence of interest in biologically inspired robotics. Biology is seen as an alternative solution to the problems robots encounter which includes algorithmic complexity, performance, and power consumption among others. The number of neurons an insect possess is approximately 10^6 while those found in a human brain are between 10^{10} and 10^{11} . Biological inspiration provides simple, yet effective methods for the solutions of such problems. The careful examination of those methods has a twofold gain. By examining the methods animals employ we can design better and more efficient robots, and by building such robots we can understand better how the mechanisms of animals work as well as how they have evolved over time.

*Currently a postdoctoral research associate within Intelligent Robot Lab, Pusan National University, Republic of Korea.

Navigation lies at the heart of mobile robotics. Homing (or inbound journey) refers to the navigation process where an autonomous agent performs a return to its home position after having completed foraging (or outbound journey; foraging is mainly attributed to a biological agent). A robot may have to return to its base for a number of reasons like recharging batteries, failure of a subsystem, or completion of a task. The application areas of robots capable of performing homing are plenty and vary. Search and rescue robots are in need in areas that have been hit by earthquakes or in environments which are hazardous for humans (Matsuno and Tadokoro, 2004). Planetary missions to other regions constitute another application area of robots whose navigation process involves returning back to their base. In this paper we have developed a novel approach to tackle the problem of robot homing using visual modality as the only source of information. No other sensor is provided to the robotic agent apart from two side cameras mounted on a simulated

mobile platform.

Optical flow, that is the rate of change of image motion in the retina or a visual sensor, is extracted from the motion of an autonomous agent. The orientation of the cameras on the robotic platform is perpendicular to the direction of motion so as a translational optical flow information is generated. Optical flow, which is not a property of the landmarks, like color, shape, and size, but of the camera motion has been used for building topological maps in *a priori* unknown environment based on the optical flow patterns of the landmarks. The novelty of our method lies in the fact that no information is given such as the position or the velocity of the robot but only the optical flow ‘fingerprint’ of the landmarks caused by the motion of the robot. For this purpose, a training algorithm has been deployed and a probability is inferred that is computed from the similarity of the optical flow patterns between the maps built during the outbound and inbound trip. The work in this paper builds upon the work of (Diamantas et al., 2010) that also appears by (Diamantas, 2010) where a single vector was modeled at varying distances and velocities. In the current work, the optical flow pattern of a landmark is modeled and its variation at varying distances and velocities is observed.

This paper is comprised of five sections. Following is Section 2 where related work is presented. In Section 3 the methodology of the homing model is described. Section 4 presents the results of the statistical model on the homing process of navigation. Finally, Section 5 epitomizes the paper with a brief discussion on the conclusions drawn from this work.

2 RELATED WORK

A large number of insects use optic flow for navigation. Insects like *Drosophila* use the apparent visual motion of objects to supply information about the three-dimensional structure of the environment. The fly *Drosophila* uses optic flow to pick near targets. (Collett, 2002) shows that the task of evaluating distances between objects is made easier by making side-to-side movements of the head strictly translational and disregarding any rotational components that can influence the distance to the objects. Looming, i.e., image expansion, can also distort the actual distance to the object as the apparent size compared to the physical size of the object differs. In his experiments (Collett, 2002) ascertains that *Drosophila* like many insects limit rotational flow during exploratory locomotion. In fact, *Drosophila* move in straight-line segments and restrict any rotation to saccades at the

end of each segment. (Schuster et al., 2002) have used virtual reality techniques to show that fruit flies use translational motion for picking up the nearest object while disregarding looming.

Ladybirds also move in straight-line segments and rely on translational optic flow rather than looming cues. Other animals like locusts and mantids turn their head from one side to the other just before jumping. (Kral and Poteser, 1997) suggest that locusts and mantids use translational motion to infer the three-dimensional structure of the environment and in particular the distance to the object they wish to approach. In some other experiments performed by (Tautz et al., 2004) trained bees had to travel large distances across various scenes that included both land and water. The results showed that the flights over water had a significantly flatter slope than the ones above land. This suggests that the perception of the distance covered by bees is not absolute but scene-dependent where the optic flow perceived is evidently larger. This may also suggest why some bees are drowning by ‘diving’ into lakes or the sea while flying above water. The distance and direction to a food source is communicated in the bees by means of waggle dances that integrate retinal image flow along the flight path (Esch et al., 2001), (von Frisch, 1993).

Experiments conducted by (Hafner, 2004) have shown that in principle visual homing strategies can be both learnt and evolved by artificial agents. Even a sparse topological representation of place cells can lead to good spatial representation of the environment where metric information can easily be extracted, if required, by the agent. Nevertheless, it is not clear which navigation strategy is applied by an animal, since its behavior consists of a combination of different strategies. When, and to what extent, the different strategies are chosen and which sensory modalities are applied is still an open question. Two well-known homing models are the *snapshot* and the *Average Landmark Vector* (ALV) model. The snapshot model is an implementation of the template hypothesis (Cartwright and Collett, 1983; Cartwright and Collett, 1987). It requires a panoramic snapshot of the goal position, be it a hive, nest, or a food source. Along with the snapshot the compass direction is stored. The snapshot model is an image matching process between a snapshot taken at a goal position and a snapshot containing the current view. The image obtained from the omnidirectional camera is unwrapped and a threshold operation is performed to yield a one-dimensional black and white image. The landmarks are denoted as black marks on the image. Then, this is compared with the snapshot of the current view to produce the homing vector. The *homing vector* is

a two-dimensional vector pointing towards the home position, and is obtained by summing up all radial and tangential vector components.

The ALV model developed by (Lambrinos et al., 2000) uses, too, a processed panoramic image but, in contrast to the snapshot model, it need not be stored. Only a two-dimensional vector for each landmark needs to be stored that points to the direction of the landmark. Matching and unwrapping of the image are not required, since the calculations are performed on the basis of vector components. Thus, ALV is more parsimonious than the snapshot model. Nevertheless, snapshots in the ALV model have to be captured and processed to produce a one-dimensional picture, as is in the snapshot model. An application of a robot with homing abilities using panoramic vision is demonstrated by (Argyros et al., 2005).

2.1 Applications of Optical Flow

Lately a growing number of autonomous vehicles have been built using techniques inspired by insects and, in particular, optic flow. One of the first works that studied the relation of scene geometry and the motion of the observer was by (Gibson, 1974). A large amount of work, however, has been focused on obstacle avoidance using optical flow (Camus et al., 1996; Warren and Fajen, 2004; Merrell et al., 2004). The technique, generally, works by splitting the image (for single camera systems) into left- and right-hand side. If the summation of vectors of either side exceeds a given threshold then the vehicle is about to collide with an object. Similarly, this method has been used for centering autonomous robots in corridors or even a canyon (Hrabar et al., 2005) with the difference that the summation of vectors this time must be equal in both the left-hand side and the right-hand side of the image. (Ohnishi and Imiya, 2007) utilize optical flow for both obstacle avoidance and corridor navigation. The performance of optical flow has also been tested in underwater color images by (Madjidi and Negahdaripour, 2006). (Vardy, 2005) employs various optical flow techniques that are compared using block matching and differential methods to tackle homing. In a recent work implemented by (Kendoul et al., 2009) optic flow is used for fully autonomous flight control of an aerial vehicle. The distance travelled in this Unmanned Aerial Vehicle (UAV) is calculated by integrating the optical flow over time. A similar work for controlling a small UAV in confined and cluttered environments has also been implemented by (Zufferey et al., 2008). (Baron et al., 1994) discuss the performance of optical flow techniques. Their comparison is focused on ac-

curacy, reliability and density of the velocity measurements. Other works employ optic flow methods for depth perception (Simpson, 1993), motion segmentation (Blackburn and Nguyen, 1995), or estimation of ego-motion (Frenz and Lappe, 2005).

A similar technique to optical flow developed by (Langer and Mann, 2003) called *optical snow* arises in situations where camera motion occurs in highly cluttered 3D environments. Such cases involve a passive observer watching the fall of the snow, hence the name of the method *optical snow*. Optical snow has been inspired by research in animals that inhabit in highly dense and cluttered environments; such animals include the rabbit, the cat, and the bird. The properties of the optical snow are that yields dense motion parallax with many depth discontinuities occurring in almost all image points. This comes in contrast to the classical methods that compute optical flow and presuppose temporal persistence and spatial coherence. (Langer and Mann, 2003) present the properties of optical snow in the Fourier domain and investigate its computational problems on motion processing.

3 METHODOLOGY

This section is dedicated to the description of the optical flow method. It is described how the optical flow 'signature' of the landmarks, that is caused by the perceived motion of the robot in the environment, can be used to localize the robot during the homing process. Various landmarks have been modeled and simulated from which the robot passes through. The simulated landmarks have geometrical shapes and they are textured in order to produce large amounts of optic flow (as is in real environments). In this work we have employed the Lucas-Kanade (LK) algorithm (Lucas and Kanade, 1981). In order for the optic flow algorithm to perform well images that have high texture and contain a multitude of corners are essential. Such images have strong derivatives and, when two orthogonal derivatives are observed then this feature may be unique, and thus, good for tracking. Tracking a feature refers to the ability of finding a feature of interest from one frame to a subsequent one. Tracking the motion of an object can give the flow of the motion of the objects among different frames. In Lucas-Kanade algorithm corners are more suitable than edges for tracking as they contain more information. For the implementation of the LK algorithm the (OpenCV, 2008) library has been used.

As mentioned in Section I the simulated robot consists of two side-ways cameras which are perpen-

dicular to the direction of motion. This creates a translational optic flow as the robot navigates through the environment. Every landmark in the environment ‘emits’ a number of optic flow vectors that are dependent on the distance between the robot and the landmark, and the velocity of the robot. One of the advantages of our method is that the images are only captured and are not used for storage or comparison. Comparing and storing only the properties of vectors between different frames reduces the computational complexity and the cost of the homing process.

During the outbound trip of the robot the camera detects and records the optic flow that is generated by the motion of the vehicle. During that phase the robot builds a topological map from the optical flow ‘fingerprint’ of the landmarks. After the foraging trip, has completed, the homing trip is initiated. In the homing phase, the robot compares the optical flow patterns it currently perceives with the ones occurred during the foraging journey. If the similarity score (i.e., probability) between the two patterns is above a given threshold, then the robot assumes the current landmark observed is the same with the landmark occurred during the outbound trip. This information is then used to localize the robot within the topological map. The similarity score of the vectors is a probabilistic result of the Euclidean distance of the vectors between the current image and the image taken during the outbound journey.

In order for the robot to localize in the environment using optic flow vectors, a training data set of $n = 1000$ observations has been implemented where the optical flow pattern of a landmark is observed at varying distances between the robot and the landmark and at varying velocities. These distances and the velocities chosen to create the training data set approximate the real distributions of velocity and distance when a robot navigates in an environment. Thus, a joint probability distribution has been created with two continuous and independent variables, that is, distance and velocity, and is expressed by (1),

$$f_{C,D}(c, d) = f_C(c) \cdot f_D(d) \quad \forall c, d. \quad (1)$$

The velocity, C , and the distance variable, D , have been drawn by two Gaussian distributions with $\mu = 4, \sigma = 1$ and $\mu = 11, \sigma = 3$ respectively. The n observations model the position of the landmark in the plane under n varying distances and velocities. One assumption that needs to be met in our method is that the majority of the vectors comprising a given landmark should have the same, or almost the same magnitude. In order to solve the matching problem between landmarks, the mean (or center) point of every vector is taken. Thus, summing up all the mean

points of the vectors and dividing by the number of vectors, v , that comprise a landmark we end up having the mean of the means as shown in (2).

$$\bar{x}, \bar{y} = \frac{1}{v} \cdot \sum_{l=1}^v x_l, y_l \quad (2)$$

The mean of the means in an optical flow pattern can be visualized as the *center of gravity* in a physical system. The same process is repeated n times where the center of gravity is observed at varying distances and velocities as shown in (3). We then compute the Euclidean distances between the center of gravity of all n observations and the center of gravity of each and every observation. Equation (4) shows the process of finding the Euclidian distances.

$$x_m, y_m = \frac{1}{n} \cdot \sum_{k=1}^n x_k, y_k \quad n = 1000 \quad (3)$$

$$d_k = \sqrt{(x_m - \bar{x}_k)^2 + (y_m - \bar{y}_k)^2} \quad (4)$$

The histogram produced by the Euclidean distances, d_k , forms a log-normal probability density function (pdf) with $\mu = 1.20$ and $\sigma = 0.71$ in the log-normal scale. In order to calculate the expected mean, $E(\mu)$, and standard deviation, $E(s.d.)$, the (5) and (6) should be used, respectively.

$$E(\mu) = e^{\mu + \frac{1}{2}\sigma^2} \quad (5)$$

$$E(s.d.) = e^{\mu + \frac{1}{2}\sigma^2} \sqrt{e^{\sigma^2} - 1} \quad (6)$$

Figure 1 shows the histogram of center of gravity deviations and the probability density function of the log-normal. The log-normal pdf is deployed in order to infer the probability a match to occur between the optical flow pattern of the current image and the optical flow pattern stored in memory. Figure 2 depicts the cumulative distribution function (cdf) of center of gravity deviations and the log-normal. The probability density function of log-normal is given by (7), and the cumulative density function of log-normal is expressed by (8), where $erfc$ is the complementary error function and Φ is the standard normal cdf.

$$f_X(\delta; \mu, \sigma) = \frac{1}{\delta\sigma\sqrt{2\pi}} e^{-\frac{(\ln\delta - \mu)^2}{2\sigma^2}} \quad \delta > 0. \quad (7)$$

$$F_X(\delta; \mu, \sigma) = \frac{1}{2} erfc \left[-\frac{\ln\delta - \mu}{\sigma\sqrt{2}} \right] = \Phi \left(\frac{\ln\delta - \mu}{\sigma} \right) \quad (8)$$

Thus far we have explained the methodology of the training algorithm. We now move on to the process of calculating a probability for the patterns observed

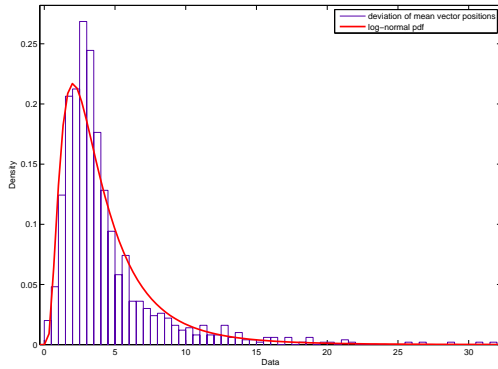


Figure 1: Histogram of center of gravity deviations of the training algorithm and the log-normal probability density function (pdf) fit. Mean and standard deviation are $\mu = 1.20$ and $\sigma = 0.71$ in the log-normal scale, respectively.

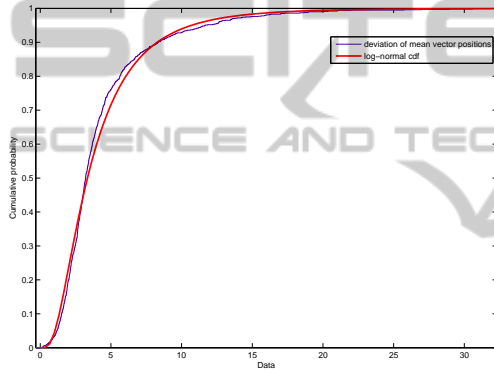


Figure 2: Cumulative density functions (cdf) of center of gravity deviations and the log-normal distribution.

by the robot during the foraging and homing process. This probability will aid the robot localize itself in the environment. During the homing navigation process, the robot calculates the mean of the means (center of gravity) from every landmark and finds their Euclidean distance δ with the mean of the means of the landmarks stored in the database. Equations (9), (10), and (11) describe the process with two distinct landmarks. In (9), (10), n and s are the number of vectors for two distinct landmarks i and j , one of which occurs in the outbound trip while the other one occurs in the inbound trip.

$$\bar{x}_i, \bar{y}_i = \frac{1}{n} \cdot \sum_{a=1}^n x_a, y_a \quad (9)$$

$$\bar{x}_j, \bar{y}_j = \frac{1}{s} \cdot \sum_{b=1}^s x_b, y_b \quad (10)$$

$$\delta = \sqrt{(\bar{x}_i - \bar{x}_j)^2 + (\bar{y}_i - \bar{y}_j)^2} \quad (11)$$

$$P = 1 - P_\delta \quad (12)$$

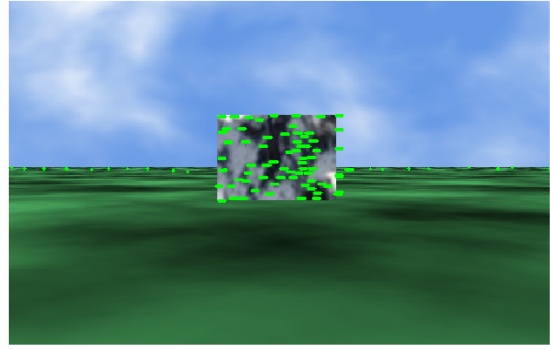


Figure 3: Reference landmark and its optical flow pattern taken at a distance of $11m$ and a velocity of $4km/h$. This reference landmark was used for comparison with other landmarks.

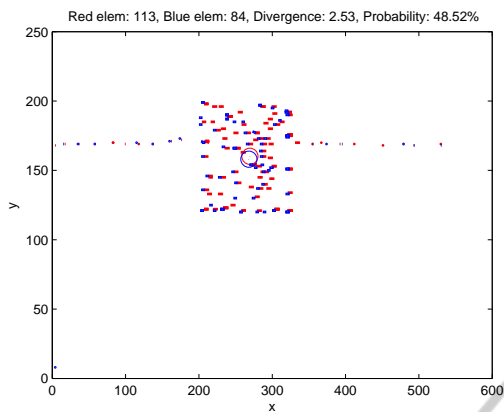
The log-normal cdf then gives us the probability P_δ based on the Euclidean distance δ between the two mean of the means. It is then subtracted from 1 to give the probability P as in (12). In addition the probability P of the log-normal is multiplied by the ratio of the number of the vectors as shown in (13),

$$P_T = P \left(\frac{\min_i}{\max_j} \right) \quad (13)$$

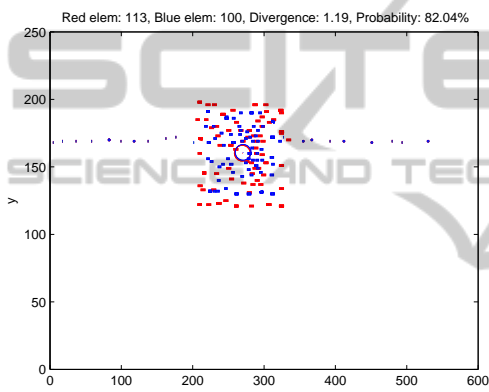
with \min_i being the landmark i with the minimum number of vectors and \max_j the maximum number of vectors of landmark j . Thus, even if the Euclidean distance between the two optical flow patterns is small, the total probability, P_T , can be low if the ratio of the vectors is small. Thus, two patterns which are totally different may have a small Euclidean distance that yields a high probability P . Multiplying this probability value by the ratio of the number of vectors can drop significantly the total probability value, P_T , assuming that the numbers of vectors are not of the same magnitude. The landmark of Fig. 3 acts as a reference for the following snapshots in order to demonstrate the similarity score at different distances and velocities, and between different landmarks. The optic flow images are produced by calculating the motion of a landmark at two time contiguous frames. It should also be noted that the flow vectors appear upside down since the images are read from top to bottom.

4 RESULTS

The homing model described in this paper has been implemented in the C++ programming language and the (MATLAB, 2007) software was used for the analysis of the data. The *breve* simulator was used for the development of the 3D environment (Klein, 2002).



(a) Optical flow pattern of the reference landmark taken at a distance of 11m and a velocity of 3km/h.

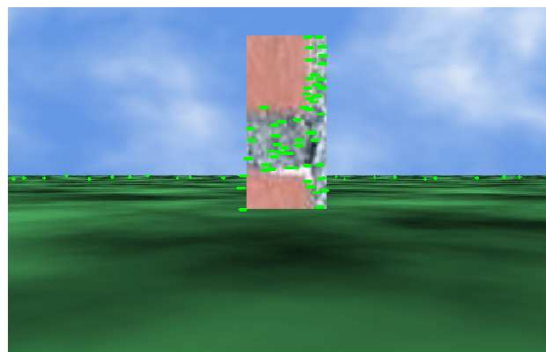


(b) Optical flow pattern of the reference landmark taken at a distance of 14m and a velocity of 4km/h.

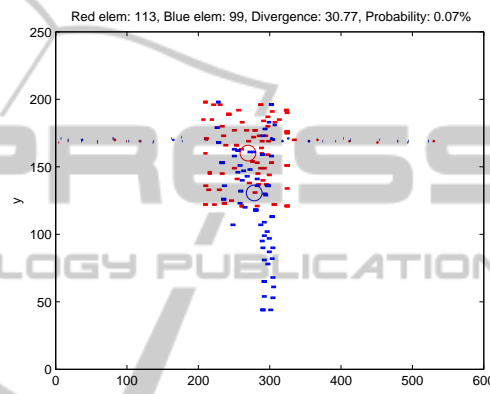
Figure 4: Optical flow patterns of the reference landmark taken at different distances and velocities.

The graphs of Fig. 4 demonstrate the effectiveness of our approach by comparing the optical flow patterns of the reference image, Fig. 3, taken at a distance of 11m and a velocity of 4km/h with the optical flow patterns of the same landmark but taken at varying distances and velocities.

The circle in the graphs represents the mean position of all the vectors that comprise a landmark, in other words the center of gravity. The red optic flow vectors refer to the reference image while the blue ones refer to the current snapshot. Vectors whose length falls below a threshold (in this case 1) are considered as outliers. Divergence is the Euclidean distance between the mean position of the vectors of the current snapshot with the mean position of the vectors of the reference image. The number of elements in the current snapshot differs from frame to frame as the angle of perception changes. From these graphs it is clear that the similarity score is quite high in both



(a) Tower-like landmark.



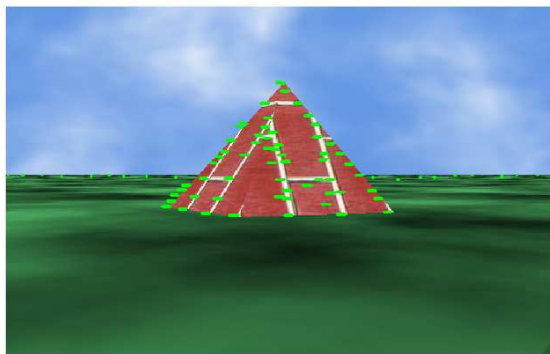
(b) Optic flow patterns between the tower-like landmark and the reference landmark.

Figure 5: Comparison of optic flow patterns between a tower-like landmark and the reference landmark. The distance of 11m remains the same as in the reference landmark as well as the velocity taken, that is 4km/h.

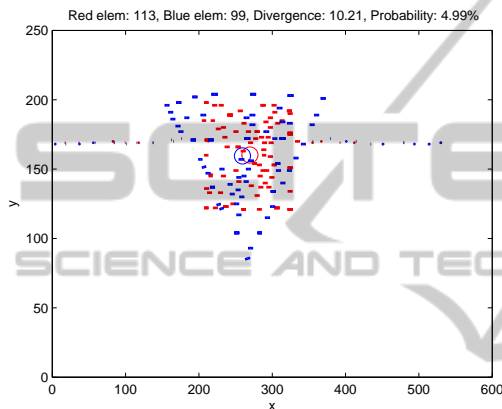
figures revealing that the same landmark has been observed when comparing the optical flow maps between the foraging and homing process. Based on this result the robot is able to localize itself using optical flow maps.

Figure 5 depicts a tower-like landmark and the reference landmark of Fig. 3. The distance and velocity at which they were captured remains the same as in the reference image, that is 11m for distance and 4km/h for velocity. In the graph of Fig. Please place \label after \caption, the similarity score is quite low, that is 0.07% while the divergence is quite high, that is 30.77. This low probability reveals that the two landmarks are different to each other.

Finally, in Fig. 6 a pyramid-like landmark is shown against the optical flow pattern of the reference landmark. In this case, too, the distance and velocity have been kept the same as in the reference landmark. The probability in Fig. Please place \label after \caption is low, too, that is 4.99% while the di-



(a) Pyramid-like landmark.



(b) Optic flow patterns between the pyramid-like landmark and the reference landmark.

Figure 6: Comparison of optic flow patterns between a pyramid-like landmark and the reference landmark. The distance of 11m remains the same as in the reference landmark as well as the velocity taken, that is 4km/h.

vergence between the centers of gravity is equal to 10.21. As in the previous example, the low probabilistic score reveals the dissimilarity of the two landmarks, even though the distance and the velocity that the images were captured are the same as in the reference landmark. It is, however, likely that two dissimilar landmarks may produce a high similarity score. This can be the case when two landmarks have similar properties such as texture, shape, and size. In such a scenario the robot will localize itself inaccurately.

5 CONCLUSIONS

In this paper we presented a novel biologically inspired method to tackle the robot homing problem. In this approach, we have considered only the optical flow patterns of the landmarks. The simulation results show that optical flow can be used as a means to perform homing. This method is parsimonious as

no other information is taken into account such as position and velocity of the robot. In addition, our method is computationally efficient as images need not be stored but the properties of the vectors, that is the mean of the means of the vectors and the number of vectors in a snapshot.

Finally, comparing the current method with the method presented by (Diamantas et al., 2010) we can infer that the method presented in this paper is more robust and accurate. In the method of (Diamantas et al., 2010) the log-normal distribution has a $\mu = 2.24$ and $\sigma = 0.86$ whereas in the current work mean and standard deviation are $\mu = 1.20$ and $\sigma = 0.71$, respectively. This biological approach may also help explain the methods employed by insects, and in particular honeybees, to perform localization and thus homing. To support this, a recent study by (Avargues-Weber et al., 2009) reveals that honeybees are capable of discriminating faces. It could well be the case of optical flow patterns.

ACKNOWLEDGEMENTS

The authors would like to thank Dr Klaus-Peter Zauer for his guidance and help in shaping the optic flow idea.

REFERENCES

- Argyros, A. A., Bekris, C., Orphanoudakis, S. C., and Kavraki, L. E. (2005). Robot homing by exploiting panoramic vision. *Journal of Autonomous Robots*, 19(1):7–25.
- Avargues-Weber, A., Portelli, G., Benard, J., Dyer, A., and Giurfa, M. (2009). Configural processing enables discrimination and categorization of face-like stimuli in honeybees. *Journal of Experimental Biology*, 213(4):593–601.
- Barron, J. L., Fleet, D. J., and Beauchemin, S. S. (1994). Performance of optical flow techniques. *International Journal of Computer Vision*, 12(1):43–77.
- Blackburn, M. and Nguyen, H. (1995). Vision based autonomous robot navigation: Motion segmentation. In *Proceedings for the Dedicated Conference on Robotics, Motion, and Machine Vision in the Automotive Industries*, pages 353–360, Stuttgart, Germany.
- Camus, T., Coombs, D., Herman, M., and Hong, T.-S. (1996). Real-time single-workstation obstacle avoidance using only wide-field flow divergence. In *Proceedings of the 13th International Conference on Pattern Recognition*, volume 3.
- Cartwright, B. and Collett, T. S. (1987). Landmark maps for honeybees. *Biological Cybernetics*, 57(1–2):85–93.

- Cartwright, B. A. and Collett, T. S. (1983). Landmark learning in bees. *Journal of Comparative Physiology A*, 151(4):521–543.
- Collett, T. (2002). Insect vision: Controlling actions through optic flow. *Current Biology*, 12(18):615–617.
- Diamantas, S. C. (2010). *Biological and Metric Maps Applied to Robot Homing*. PhD thesis, School of Electronics and Computer Science, University of Southampton.
- Diamantas, S. C., Oikonomidis, A., and Crowder, R. M. (2010). Towards optical flow-based robotic homing. In *Proceedings of the International Joint Conference on Neural Networks (IEEE World Congress on Computational Intelligence)*, pages 1–9, Barcelona, Spain.
- Esch, H., Zhang, S., Srinivasan, M., and Tautz, J. (2001). Honeybee dances communicate distances measured by optic flow. *Nature*, 411(6837):581–583.
- Frenz, H. and Lappe, M. (2005). Absolute travel distance from optic flow. *Vision Research*, 45(13):1679–1692.
- Gibson, J. J. (1974). *The Perception of the Visual World*. Greenwood Publishing Group, Santa Barbara, CA, USA.
- Hafner, V. V. (2004). *Adaptive navigation strategies in biorobotics: Visual homing and cognitive mapping in animals and machines*. Shaker Verlag GmbH, Aachen.
- Hrabar, S., Sukhatme, G., Corke, P., Usher, K., and Roberts, J. (2005). Combined optic-flow and stereo-based navigation of urban canyons for a UAV. In *Proceedings of IEEE/RSJ International Conference on Intelligent Robots and Systems*, pages 302–309.
- Kendoul, F., Fantoni, I., and Nonami, K. (2009). Optic flow-based vision system for autonomous 3D localization and control of small aerial vehicles. *Robotics and Autonomous Systems*, 57(6–7):591–602.
- Klein, J. (2002). Breve: A 3D simulation environment for the simulation of decentralized systems and artificial life. In *Proceedings of Artificial Life VIII, the 8th International Conference on the Simulation and Synthesis of Living Systems*.
- Kral, K. and Poteser, M. (1997). Motion parallax as a source of distance information in locusts and mantids. *Journal of Insect Behavior*, 10(1):145–163.
- Lambrinos, D., Moller, R., Labhart, T., Pfeifer, R., and Wehner, R. (2000). A mobile robot employing insect strategies for navigation. *Robotics and Autonomous Systems, special issue: Biomimetic Robots*, 30(1–2):39–64.
- Langer, M. and Mann, R. (2003). Optical snow. *International Journal of Computer Vision*, 55(1):55–71.
- Lucas, B. D. and Kanade, T. (1981). An iterative image registration technique with an application to stereo vision. In *Proceedings of the 7th International Joint Conference on Artificial Intelligence (IJCAI), August 24–28*, pages 674–679.
- Madjidi, H. and Negahdaripour, S. (2006). On robustness and localization accuracy of optical flow computation for underwater color images. *Computer Vision and Image Understanding*, 104(1):61–76.
- MATLAB (2007). <http://www.mathworks.com/>.
- Matsuno, F. and Tadokoro, S. (2004). Rescue robots and systems in Japan. In *IEEE International Conference on Robotics and Biomimetics*, pages 12–20.
- Merrell, P. C., Lee, D.-J., and Beard, R. (2004). Obstacle avoidance for unmanned air vehicles using optical flow probability distributions. *Sensing and Perception*, 5609:13–22.
- Ohnishi, N. and Imiya, A. (2007). Corridor navigation and obstacle avoidance using visual potential for mobile robot. In *Proceedings of the Fourth Canadian Conference on Computer and Robot Vision*, pages 131–138.
- OpenCV (2008). <http://opencv.willowgarage.com/wiki/>.
- Schuster, S., Strauss, R., and Gotz, K. G. (2002). Virtual-reality techniques resolve the visual cues used by fruit flies to evaluate object distances. *Current Biology*, 12(18):1591–1594.
- Simpson, W. (1993). Optic flow and depth perception. *Spatial Vision*, 7(1):35–75.
- Tautz, J., Zhang, S., Spaethe, J., Brockmann, A., Si, A., and Srinivasan, M. (2004). Honeybee odometry: Performance in varying natural terrain. *Plos Biology*, 2(7):915–923.
- Vardy, A. (2005). *Biologically Plausible Methods for Robot Visual Homing*. PhD thesis, School of Computer Science, Carleton University.
- von Frisch, K. (1993). *The Dance Language and Orientation of Bees*. Harvard University Press, Cambridge, MA, USA.
- Warren, W. and Fajen, B. R. (2004). From optic flow to laws of control. In Vaina, L. M., Beardsley, S. A., and Rushton, S. K., editors, *Optic Flow and Beyond*, pages 307–337. Kluwer Academic Publishers.
- Zufferey, J.-C., Beyeler, A., and Floreano, D. (2008). Optic flow to control small UAVs. In *IEEE/RSJ International Conference on Intelligent Robots and Systems: Workshop on Visual Guidance Systems for small autonomous aerial vehicles*, Nice, France.